

# A new methodology to determine kinetic parameters for one- and two-step chemical models

By T. Mantel<sup>1</sup>, F. N. Egolfopoulos<sup>2</sup> & C. T. Bowman<sup>3</sup>

In this paper, a new methodology to determine kinetic parameters for simple chemical models and simple transport properties classically used in DNS of premixed combustion is presented. First, a one-dimensional code is utilized to perform steady unstrained laminar methane-air flame in order to verify intrinsic features of laminar flames such as burning velocity and temperature and concentration profiles. Second, the flame response to steady and unsteady strain in the opposed jet configuration is numerically investigated. It appears that for a well determined set of parameters, one- and two-step mechanisms reproduce the extinction limit of a laminar flame submitted to a steady strain. Computations with the GRI-mech mechanism (177 reactions, 32 species) and multicomponent transport properties are used to validate these simplified models. A sensitivity analysis of the preferential diffusion of heat and reactants when the Lewis number is close to unity indicates that the response of the flame to an oscillating strain is very sensitive to this number. As an application of this methodology, the interaction between a two-dimensional vortex pair and a premixed laminar flame is performed by DNS using the one- and two-step mechanisms. Comparison with the experimental results of Samaniego *et al.* (1994) shows a significant improvement in the description of the interaction when the two-step model is used.

---

## 1. Introduction

During the past ten years, direct numerical simulation (DNS) of turbulent reacting flows has been widely utilized to obtain physical understanding and precious information for modeling purposes. The recent articles of Poinso (1996) and Poinso *et al.* (1996) can be consulted for a review concerning DNS of turbulent reacting flows. Although any kind of model is needed to solve the Navier-Stokes equations for a non-reacting system, closures have to be provided in order to model transport properties of the different species and chemical reactions as well. These two aspects can rapidly lead to tremendous needs of storage capacity and CPU time even for the combustion of simple hydrocarbons such as methane. As an example, the recent detailed mechanism proposed by the Gas Research Institute (GRI) for methane combustion requires 177 reactions of 32 species. This kind of chemical scheme can only be used in the computations of one-dimensional problems such as the study

<sup>1</sup> Renault, Research Division, France

<sup>2</sup> University of Southern California, Department of Mechanical Engineering

<sup>3</sup> Stanford University

of strained laminar premixed flames (Egolfopoulos 1994a-b). We can, however, cite the two-dimensional numerical study of vortex-premixed laminar flame interactions performed by Hilka *et al.* (1994) using a detailed mechanism (17 species and 55 reactions). Thus, in order to investigate turbulent flames propagating in the combustion regime of existing devices, the chemistry and transport properties have to be drastically simplified. Currently, a one-step irreversible chemical model is used to performed parametric studies of complex flows such as flame-vortex interactions (Poinso *et al.* 1991), three-dimensional decaying turbulence interacting with a premixed flame (Trouvé & Poinso 1994), or a diffusion flame (Vervisch 1992). In order to take into account the highly diffusive behavior of some radicals, two-step mechanisms have been used in numerical studies of turbulent diffusion flames (Vervisch 1992) and flame-vortex interactions (Mantel 1994). The difficulty of these simple models is to find realistic transport properties and kinetic parameters which correspond to the studied medium. In the DNS code used by these various authors, the transport properties are modeled using a temperature dependence for the dynamic viscosity and constant Prandtl, Schmidt numbers, and calorific capacity. For the chemical models, the activation energy  $E_a$  and frequency factor  $B$  for each reaction have to be estimated. Usually, a high activation energy in the range of 30 to 60 kcal/mol is considered. For premixed systems, the kinetic parameter of these simple chemical models are chosen to match the laminar burning velocity  $S_L$  alone. An *a priori* global activation energy must be taken high enough to be realistic but low enough to reduce the number of grid points required to resolve the flame (generally the lower limit of the range 30 to 60 kcal/mol). In fact, the asymptotic analysis of Williams (1985) shows that  $\delta_f \sim \beta^{-1}$  where  $\delta_f$  is the thickness of the reaction zone and  $\beta$  the Zel'dovich number defined by  $\beta = E_a(T_b - T_u)/R^o T_b^2$ . Here,  $R^o$ ,  $T_u$ , and  $T_b$  represent respectively the universal gas constant and the temperature of the fresh and burnt gases. Once the activation energy is imposed, the frequency factor is tuned to find the chosen laminar flame velocity. However, since an infinity of couple  $(B, E_a)$  exists for a given value of  $S_L$ , additional features of the laminar flame have to be verified. Thus, this technique has to be improved in order to predict other intrinsic characteristics of the flame such as concentration of reactants and temperature profiles, especially in the downstream end of the flame where reactions take place.

The motivation of this study is to provide realistic kinetic parameters for one- and two-step mechanisms classically used in DNS of premixed turbulent combustion. To do so, a new methodology allowing the determination of kinetic parameters is proposed. This methodology allows to verify the following quantities: (1) the laminar burning velocity, (2) the temperature and concentration of reactant (and intermediate species for the two-step mechanism) profiles, and (3) the strain rate imposed to the flame in the opposed jet flame configuration leading to extinction .

Points 1 and 2 are performed using the PREMIX code (Kee *et al.* 1994), which has been modified to accept artificial species, constant molecular weight, constant calorific capacities for all the species, and modified heat of formation to predict the adiabatic flame temperature. Point 3 is numerically investigated by studying

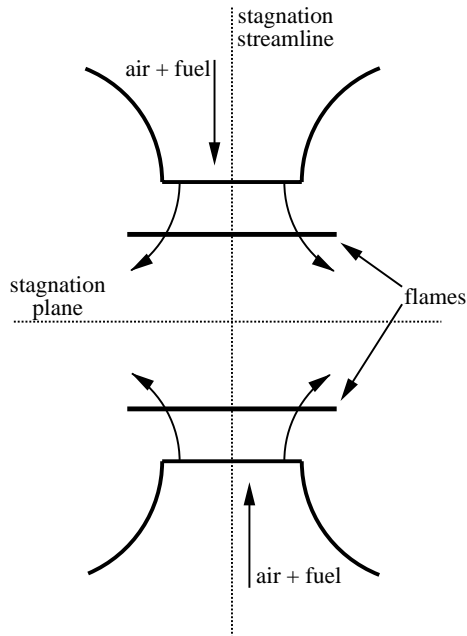


FIGURE 1. Counterflow flame configuration.

the counterflow opposed jet flame configuration (Egolfopoulos 1994). For these 3 points, computations using the GRI-mech 2.1 mechanism (Frenklach *et al.* 1995) are performed and utilized as reference cases for comparison with one- and two-step mechanisms.

In order to validate this methodology on real configurations, the response of a premixed laminar flame to unsteady strain is numerically investigated in two different configurations using one- and two-step chemical models and simple transport properties:

- the opposed jet flame submitted to an oscillating strain rate
- the vortex-premixed laminar flame interaction experimentally studied by Samaniego *et al.* (1996)

In the first unsteady configuration, the effect of thermo-diffusive properties of the mixture is investigated. It appears that this effect seems to have a strong influence on the unsteady behavior of the heat release rate. On this configuration, both one- and two-step models allow a good description of the behavior of the flame. In the case of the vortex-premixed laminar flame interaction, a significant effect of the diffusivity of the intermediate species on the heat release is observed when the two-step mechanism is employed. Comparison with the experimental results of Samaniego *et al.* (1996) shows an improvement in the description of the interaction using the two-step model and simplified transport model.

## 2. Lean premixed laminar flames submitted to a steady strain

### 2.1 Presentation of the counterflow flame configuration

To study the ability of one- and two-step models to describe the response of a laminar flame to stretch, the counterflow flame interaction configuration is chosen.

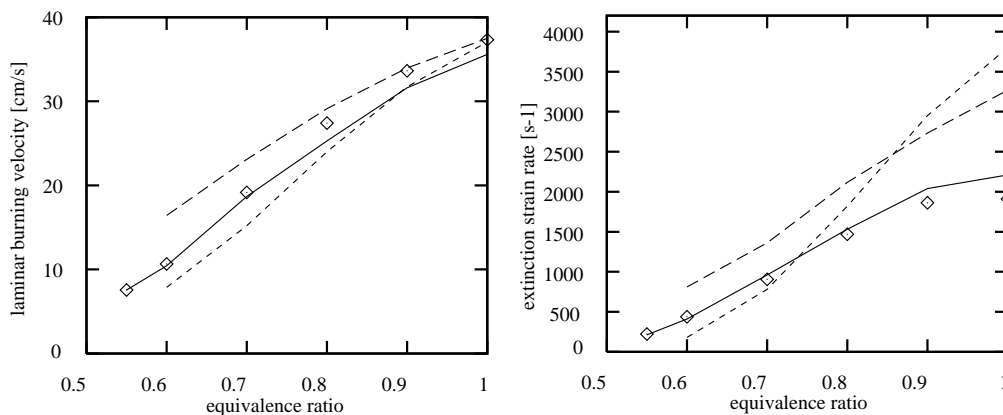


FIGURE 2. Evolution of the laminar burning velocity and extinction strain rate versus the equivalence ratio.  $\diamond$  : GRI-mech; — : model; ---- :  $E_a = 35\text{kcal/mol}$ ; -.-.- :  $E_a = 60\text{kcal/mol}$ .

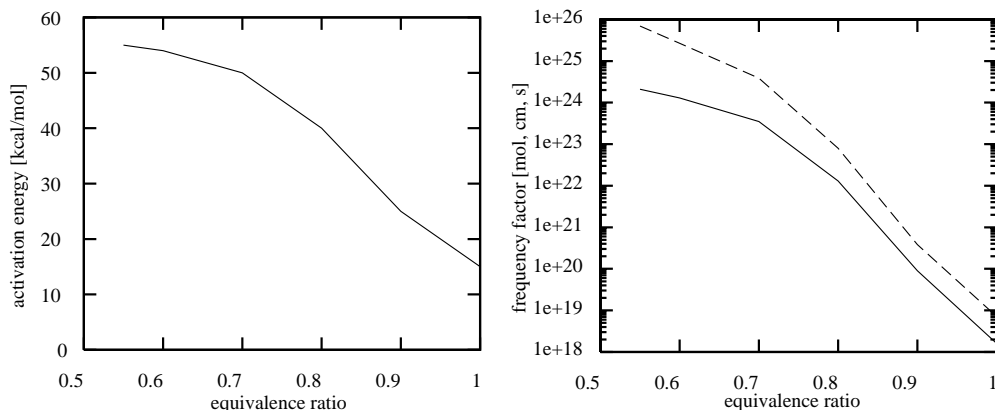


FIGURE 3. Evolution of the activation energy in kcal/mol and frequency factor in mol, cm, s for reaction (1) versus the equivalence ratio. — : PREMIX code; ---- : asymptotic analysis.

Such a configuration (see Fig. 1) has been widely studied both experimentally (Chung *et al.* 1986, Law *et al.* 1986) and numerically (Egolfopoulos 1994a,b). The main goal of these studies was to determine the extinction and flammability limits of laminar premixed flames. Extinction strain rates and laminar flame velocity have been determined for a wide range of equivalence ratio for various air/fuel mixtures for premixed laminar.

Here, this problem is treated using a code solving the equations of mass, momentum, energy, and species along the stagnation streamline of the counterflow opposed jet flame configuration. Details concerning the equations and boundary conditions are given in Egolfopoulos (1994a).

The conditions of our simulations are those retained by Egolfopoulos (1994). The temperature of the unburnt mixture (methane-air) is 300 K, and the distance separating the nozzles is 0.7 cm.

## 2.2 A one-step model for the combustion of lean methane-oxygen flames

A new model for the combustion of lean methane-air flame is proposed following the methodology presented in the introduction. The global one-step reaction for lean methane-air combustion is:



and the reaction rate for this reaction is expressed by

$$RR = B[\text{CH}_4][\text{O}_2]^2 \exp(-E_a/R^oT) \quad (2)$$

Computations are performed using the PREMIX code including reaction (1) and multi-component properties. The parameters  $B$  and  $E_a$  are thus determined for each value of the equivalence ratio  $\phi$ . Figure (2) shows the evolution of  $S_L$  and  $K_{ext}$  for the global mechanism and for the solution obtained from the GRI-mech mechanism. The values for  $B$  and  $E_a$  are presented in Table (1) as a function of  $\phi$  varying from 0.55 to 1.

Two additional cases are presented in Fig. (2) by keeping constant kinetic parameters: (i)  $E_a = 35$  kcal/mol;  $B = 4.1 \cdot 10^{21}$  (ii)  $E_a = 60$  kcal/mol;  $B = 6 \cdot 10^{24}$ . These sets of parameters are determined for  $\phi = 1.0$  and are kept constant for the other values of  $\Phi$ . For these two cases, both  $S_L$  and  $K_{ext}$  are not correctly predicted. For some values of  $\phi$ ,  $K_{ext}$  is even over-predicted by a factor of two (see Fig 2).

$\phi$	$E_a$ kcal/mol	$\Lambda$ cm/(mol s)
0.55	55	$2.1 \cdot 10^{24}$
0.6	54	$1.1 \cdot 10^{24}$
0.7	50	$3.1 \cdot 10^{23}$
0.8	40	$1.1 \cdot 10^{22}$
0.9	25	$9.1 \cdot 10^{19}$
1.0	15	$1.1 \cdot 10^{18}$

Table 1. Kinetics parameters for global reaction defined by Eq. (1) used in Fig. (1)

The evolution of  $B$  as a function of  $\phi$  obtained in the present study can be compared with the asymptotic analysis of Clavin (1985), who proposes an expression for the laminar burning velocity  $S_L$  as a function of  $B$  and  $\beta$ :

$$S_L = \frac{\rho_b}{\rho_u} \left[ 2\Gamma_{n+1} L e^n \frac{D_{th}(T_b)}{\beta^{n+1} \tau_r} \right]^{1/2} \quad (3)$$

where

$$\Gamma_{n+1} = \int_0^\infty X^n e^{-X} dX \quad (4)$$

$$\frac{1}{\tau_r} = \nu \frac{W}{Y_u} B C_{o,u}^{n_o} C_{f,u}^{n_f} \exp(-\beta/\alpha) \quad (5)$$

Here,  $\nu$ ,  $Y_u$ ,  $W$  are the stoichiometric coefficient, the initial mass fraction, and the molecular mass of the deficient species. The molar concentration of the oxidant and the fuel in the fresh mixture are denoted by  $C_{o,u}^{n_o}$  and  $C_{f,u}^{n_f}$ . In Eq. (4),  $n$  is the order of the reaction and  $X$  a variable of integration defined by  $X = \beta(1 - \theta)$  where  $\theta = (T - T_u)/(T_b - T_u)$  represents the reduced temperature.

In the case of the global reaction (1), Eqs. (4) and (5) become:

$$\Gamma = 2 \quad (6)$$

$$\frac{1}{\tau_r} = \nu_{CH_4} \frac{W_{CH_4}}{Y_{CH_4,u}} B C_{O_2,u}^2 C_{CH_4,2} \exp(-\beta/\alpha) \quad (7)$$

To estimate the thermal diffusivity in the burnt gases, we use the classical relation:

$$\frac{\mu}{\mu_u} = \left( \frac{T}{T_u} \right)^b \quad (8)$$

with  $b = 0.76$ .

Reporting Eqs. (6-8) into Eq. (3), we obtain:

$$B = \frac{1}{4} S_L^2 \frac{Pr W_{O_2}^2}{\rho_u^2 Y_{O_2,u}^2 \nu_{CH_4}} (1 - \alpha)^{b-1} \beta^3 \exp(\beta/\alpha) \quad (9)$$

Due to the assumptions used in the asymptotic analysis (constant calorific capacities, thermal, and species diffusivities), Eq. (9) constitutes a first approximation for  $B$ . The values for  $B$  given by Eq. (9) are compared with the result obtained using PREMIX. Asymptotic analysis exhibits higher values for  $B$  compared to PREMIX. This is also noticed by Rutland (1989), who studied the propagation of a one-dimensional premixed laminar flame using a one-step chemical model and by considering constant transport properties.

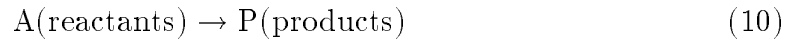
### 2.3 Kinetics parameters of one- & two-step models for lean premixed laminar flame

In this section, the kinetic parameters for one- and two-step models are determined for the combustion of a methane-air premixed laminar flame with an equivalence ratio of 0.55 using the PREMIX code. Particular conditions for the transport properties are considered. The dynamic viscosity is expressed according Eq. (8) and constant Prandtl and Schmidt numbers are assumed. Calorific capacity is also assumed constant and the molecular weights of all the species are equal. To do so, the PREMIX code had to be modified to accept artificial species and modified transport properties.

The motivations of these choices are directly related to the DNS code applied to complex flows such as vortex-premixed flame or turbulence-premixed flame interactions.

### 2.3.1 The one-step model chemical model

In this model, the chemistry is described by a single step irreversible reaction:



The reaction rate of this reaction is expressed using a classical Arrhenius law

$$\dot{w}_A = BC_A \exp(-E_a/R_oT) \quad (11)$$

For this simplest chemical model, 4 parameters appear:  $B$ ,  $E_a$ ,  $(\Delta H)$ , and  $Le_A$  ( $(\Delta H)$  being the heat released by the reaction). Since  $Le_A$  and  $(\Delta H)$  can easily be determined (by using binary diffusion coefficient for the Lewis number and by matching the fully burnt gas temperature for  $(\Delta H)$ ), we have to determine  $B$  and  $E_a$ .

### 2.3.2 The two-step chemical model

The two-step mechanism initially proposed by Zel'dovich (1948) consists of a first order chain branching reaction and a second-order termination reaction:



The use of a two-step mechanism significantly increases the number of unknowns. Now, 8 parameters have to be determined:  $B_1$ ,  $B_2$ ,  $E_{a_1}$ ,  $E_{a_2}$ ,  $(\Delta H)_1$ ,  $(\Delta H)_2$ ,  $Le_A$ , and  $Le_X$  where  $(\Delta H)_1$  and  $(\Delta H)_2$  represent the heat released by the first and by the second reaction. To reduce the number of unknowns, some realistic assumptions can be proposed:

- the first reaction has a high activation energy and is thermo-neutral (Liñán 1974)
- the second reaction has a zero activation energy and liberates all the heat (Liñán 1974) coefficients

These assumptions lead to simplified expression for the reaction rates of the reactions (12) and (13).

$$RR_1 = B_1 C_A C_X \exp(-E_{a_1}/R_oT) \quad (14)$$

$$RR_2 = B_2 C_X^2 \quad (15)$$

Moreover, since the H atom provides a crucial source of radicals and plays a determining role in the submechanism  $H_2 - O_2$  (Glassman 1987), we relate the intermediate species of the two-step mechanism to the H atom. Thus, from binary diffusion coefficients, the Lewis numbers for A and X are:  $Le_A = 1.0$ ,  $Le_X = 0.15$ . From these considerations, 3 parameters still have to be determined:  $B_1$ ,  $B_2$ , and  $E_{a_1}$ .

To determine the remaining unknowns of the one- and two-step mechanisms, the methodology previously described is applied.

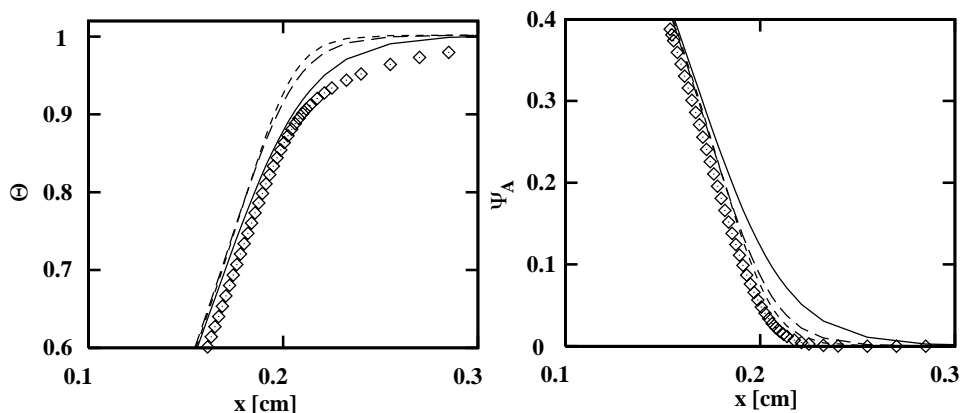


FIGURE 4. Temperature and A mass fraction obtained with the one-step model (reduced by its value in the fresh gas) at the trailing edge of the flame.  $\diamond$  : GRI-mech ( $\text{CH}_4$  mass fraction); — :  $E_a = 30\text{kcal/mol}$ - $B = 1.82e8$ ; - - - :  $E_a = 45\text{kcal/mol}$ - $4.93e10$ ; - · - · :  $E_a = 60\text{kcal/mol}$ - $B = 1e13$  ( $B$  in mol, s).

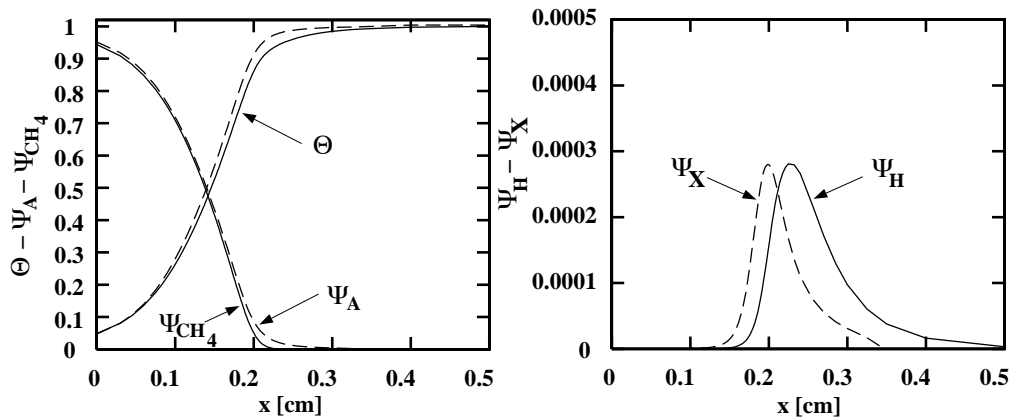


FIGURE 5. Reduced methane and H concentration and temperature profiles across the laminar flame front. — : GRI-mech; - - - : two-step mechanism.

### 2.3.3 Results

First, the influence of kinetic parameters of one- and two-step models on the flame structure is analyzed. The flame structure is very sensitive to the couple  $(B, E_a)$  especially in the trailing edge of the flame (see Fig. 4). Since both  $B$  and  $E_a$  vary, it is difficult to know which of these two parameters influences the gradients of temperature and concentration. The profiles of  $\Psi_{\text{CH}_4} = Y_{\text{CH}_4}/Y_{\text{CH}_4,u}$  in the burnt gas side seems to be very critical in the opposed jet configuration. When the flames interact between them, incomplete combustion by leakage of the fuel can lead to sudden extinction. This is particularly true for the case  $E_a = 30\text{ kcal/mol}$ ,  $B = 1.82 \cdot 10^8\text{ mol}^{-1}\text{s}^{-1}$  for which the spreading of the  $\text{CH}_4$  profile is more pronounced. For these values, the one-step model predicts an extinction strain rate of  $50\text{s}^{-1}$ , whereas the experimental results give  $K_{exp} = 200\text{s}^{-1}$  (Egolfopoulos 1994a).

This can be explained by noticing that for high activation energy, the thin reaction

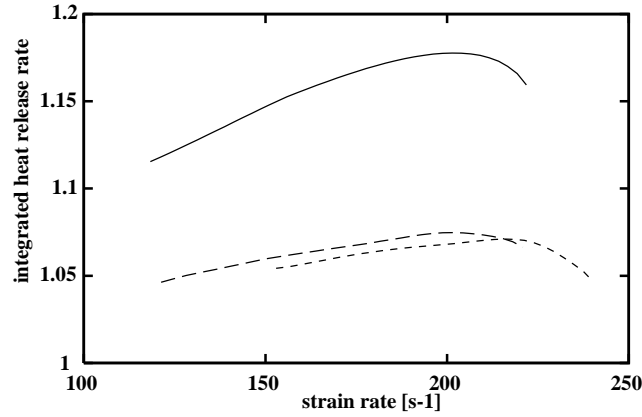


FIGURE 6. Evolution of the heat release integrated across the flame front (reduced by the unstrained value) in function of the strain. — : GRI-mech; ---- : one-step mechanism; -.-.- : two-step mechanism.

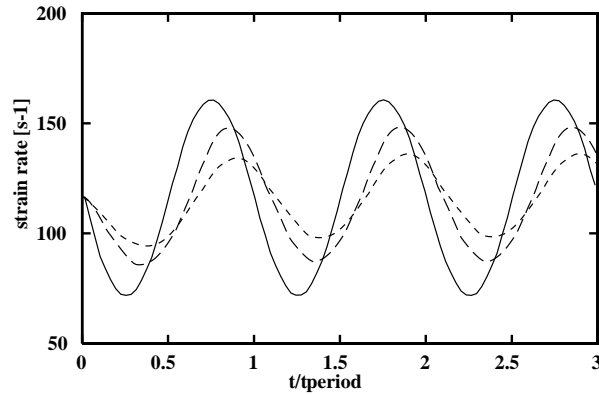


FIGURE 7. Evolution of the strain rate in function of time for different frequencies. — : 1 Hz; ---- : 40 Hz; -.-.- : 80 Hz.

zone is located at the downstream end of the temperature and concentration profiles (since the reaction zone is proportional to  $\beta^{-1}$ ). Thus, for larger values of  $E_a$ , low strain rates only affect the preheat zone. As the strain rate increases, the temperature and concentration profiles are steeper, and the reaction zone starts to be affected by the strain. This effect is emphasized in the twin flame configuration where the distance separating the two reaction zones is a key parameter in the processes leading to extinction. The determination of the extinction strain rate (in the opposed jet configuration) depends directly on the good prediction of the position of the reaction zone in function of the inlet mass flow rate and, consequently, the strain rate.

Figure (5) represents the flame structure using the two-step mechanism. Here, the concentration of the intermediate species is also of interest because of the quadratic dependence on  $Y_X$  on the heat release rate (see Eq. 15). The maximum value of  $X$  is chosen by matching the maximum value of the H atom concentration given by the GRI mechanism. Once  $B_1$  and  $E_{a_1}$  are chosen to match the  $\theta$  and  $\Psi_A$  profiles, the

maximum of  $\Psi_X$  is directly related to the frequency factor of the second reaction  $B_2$ . We also observe a space shift of the  $\Psi_X$  compared to the  $\Psi_H$  profile. This could be overcome by decreasing  $B_1$  in order to change the production of X. However, the decrease of  $B_1$  directly leads to a thickening of the flame in the burnt gas side of the flame and, consequently, to a different response of the flame to strain. Thus, a compromise between the profiles of  $\theta$ ,  $\Psi_A$ , and  $\Psi_X$  has to be found in order to obtain the right extinction strain rate in the opposed jet flame configuration. Finally, Fig. (6) shows the flame response to a steady strain rate obtained for the one- and two-step models and the comparison with the solution given by the GRI mechanism. Here, the heat release rate integrated across the flame (normalized by the unstrained value) is presented. Both the one- and two-step mechanisms allow us to find the correct extinction strain rate (within 10% of error). We also notice that the Lewis number effect is also observed by using the simple transport properties described in section (2.3). Since the Lewis number based on the limiting species (here  $\text{CH}_4$ ) is less than unity ( $Le_A = 0.95$ ), a positive stretch applied to the flame increases the heat release. As the stretch increases, the reaction zones are pushed toward the stagnation plane, and reaction cannot be sustained due to shorter residence time (Law 1988).

### 3. Lean premixed laminar flames submitted to an oscillating strain

#### 3.1 Analysis of the flame response

The response of a laminar premixed methane-air flame to unsteady strain is numerically studied using one- and two step chemical models. The unsteadiness of the flow is obtained by imposing a sinusoidal velocity field at the inlet boundaries. The amplitude of the velocity variations is 20% of the mean value inlet velocity. Three different frequencies for the velocity fluctuations are studied (1, 40, and 80 Hz). The strain rate applied to the flame varies from 70 to 160  $\text{s}^{-1}$ , corresponding to Karlovitz number varying from 0.33 to 0.75. Here, the Karlovitz number is defined by  $Ka = \tau_c K$  where  $K$  is the strain rate and  $\tau_c$  a chemical time scale defined by  $\tau_c = \alpha_u/S_L^2$ ,  $\alpha_u$  being the thermal diffusivity in the fresh gases. The order of magnitude of the Karlovitz number is typically representative of the flamelet regime defined by the Klimov-Williams criteria ( $Ka < 1$ ).

The time evolution of the heat release rate integrated across the flame (non-dimensionalized by the unstrained value) is presented Fig. (8). As a first observation, no phase shift is observed between the one- and two-step chemical models and the solution given by the GRI mechanism. The slight asymmetry between the slopes corresponding to the extension and relaxation observed by the GRI mechanism is also described by the two-step model. Figure (9) represents the heat release amplitude (normalized by its steady strained value) for different frequencies. The amplitudes of the fluctuations are underestimated by the simple models even if the tendency is well reproduced. As previously observed by Egolfopoulos (1994a), at low frequencies the flame behaves like in the steady case whereas at higher frequencies, the amplitude of the fluctuations decreases. The attenuation of the heat release amplitude at higher frequencies is explained by the fact that the disturbances are

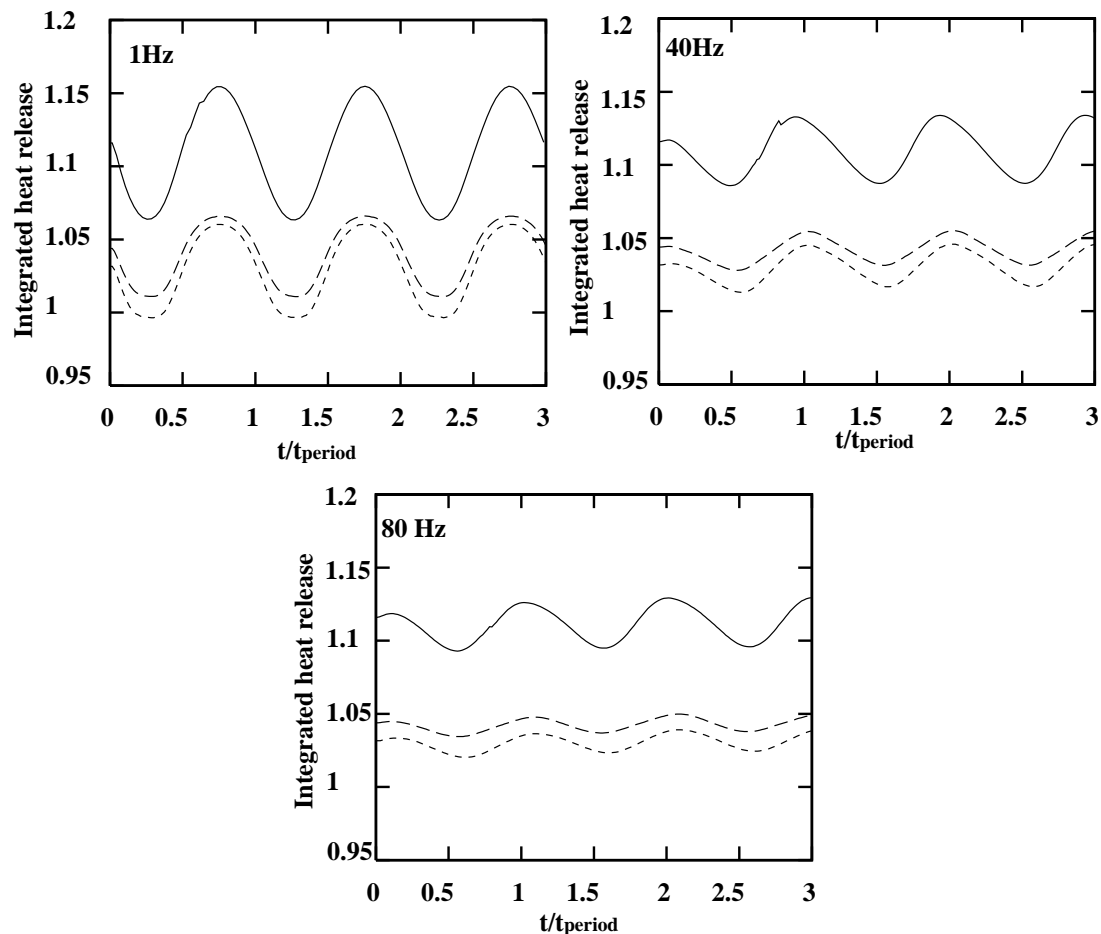


FIGURE 8. Evolution of the heat release integrated across the flame front (reduced by the unstrained value) in function of time ( $Le_A = 0.95$ ). — : GRI-mech; ---- : one-step mechanism; ..... : two-step mechanism.

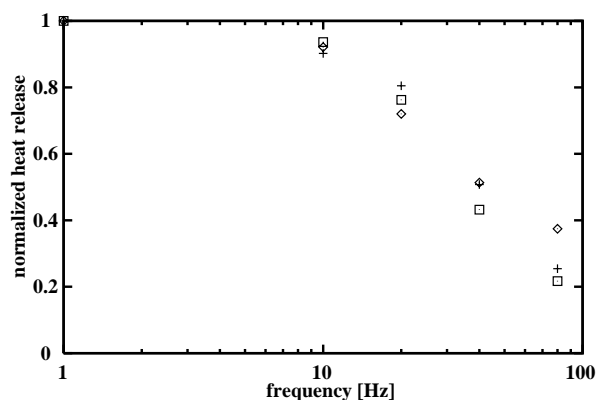


FIGURE 9. Evolution of the heat release amplitude (normalized by its unstrained value) in function of the frequency.  $\diamond$  : GRI-mech; + : one-step mechanism;  $\square$  : two-step mechanism.

rapidly attenuated by diffusion effects (Egolfopoulos 1994a).

### 3.2 Response of a flame with unity Lewis number to an oscillating strain

We also notice that the heat release rate given by the two-step mechanism is always lower than the results given by the one-step mechanism. This can be explained using the asymptotic analysis of Seshadri & Peters (1983) who studied the structure of a planar premixed laminar flame submitted to stretch. Considering a high activation energy for the first reaction, the authors derived an asymptotic expansion for the temperature. They found that the first order temperature can be expressed as a function of stretch and Lewis numbers for the reactant and the intermediate species:

$$T_0^1 = -K^* \left\{ \frac{Le_A - 1}{Le_A} + (-\Delta H_2^*) \left[ \frac{1 - Le_X}{Le_X} I_0 \right] + \frac{Y_{X_0}^1}{Le_X} \right\} \quad (16)$$

The subscript 0 refers to the axial coordinate where  $Y_X$  is maximum,  $I_0$  is a function always positive,  $K^*$  is a non-dimensionalized stretch, and  $(-\Delta H_2^*)$  is the non-dimensionalized heat of reaction of the recombination step. The relation (16) points out the respective roles of the diffusivities of the reactant and of the intermediate species. Considering only the first term on the RHS of Eq. (16), for positive stretch the temperature increases for  $Le_A < 1$ . For  $Le_A = 1$ , the temperature remains constant equal to the zero order temperature regardless the value of the stretch. This recovers the classical conclusions of the role played by the Lewis number of the reactant on the dynamic of stretched flames (Clavin 1985, Law 1988). The second term on the RHS of (16) enhances the effects of diffusivity of the intermediate species on the dynamic of stretched flames. Since radicals are mostly very light species, they have high diffusivities leading to Lewis numbers significantly less than unity (here  $Le_X = 0.15$ ). Thus, in the case of positive stretch, the diffusivity of the intermediate species tends to decrease the temperature and, consequently, the local laminar flame speed. This result points out that even for  $Le_A = 1$  the flame can be sensitive to stretch effect and exhibits local variations of the laminar flame speed not only due to compression of the reaction zone.

Moreover, under some circumstances, a positive stretch can produce a decrease of the heat release rate when the Lewis number of the reactant is slightly less than unity. This is observed in Fig. (8) for the frequency 1 Hz and  $Le_A = 0.95$  where the normalized heat release rate goes under unity.

In order to characterize the effect of a slight variation of the Lewis number, the response of the flame to unsteady strain is analyzed by imposing the Lewis number for the reactant equal to unity. This slight variation of  $Le_A$  has a strong consequence on the flame response. Figure 10 shows the evolution of the heat release integrated across the flame front for  $Le_A = 1.0$  and for 1, 40, and 80 Hz. The results issued from the one- and two-step calculations are in opposition of phase compared to the solution given by the GRI mechanism. Due to the compression of the reaction zone, the integrated heat release is less than unity for both one- and two step-models. Moreover, for the two-step mechanism, the diffusion of the intermediate species also contributes to the decrease of the heat release as previously explained.

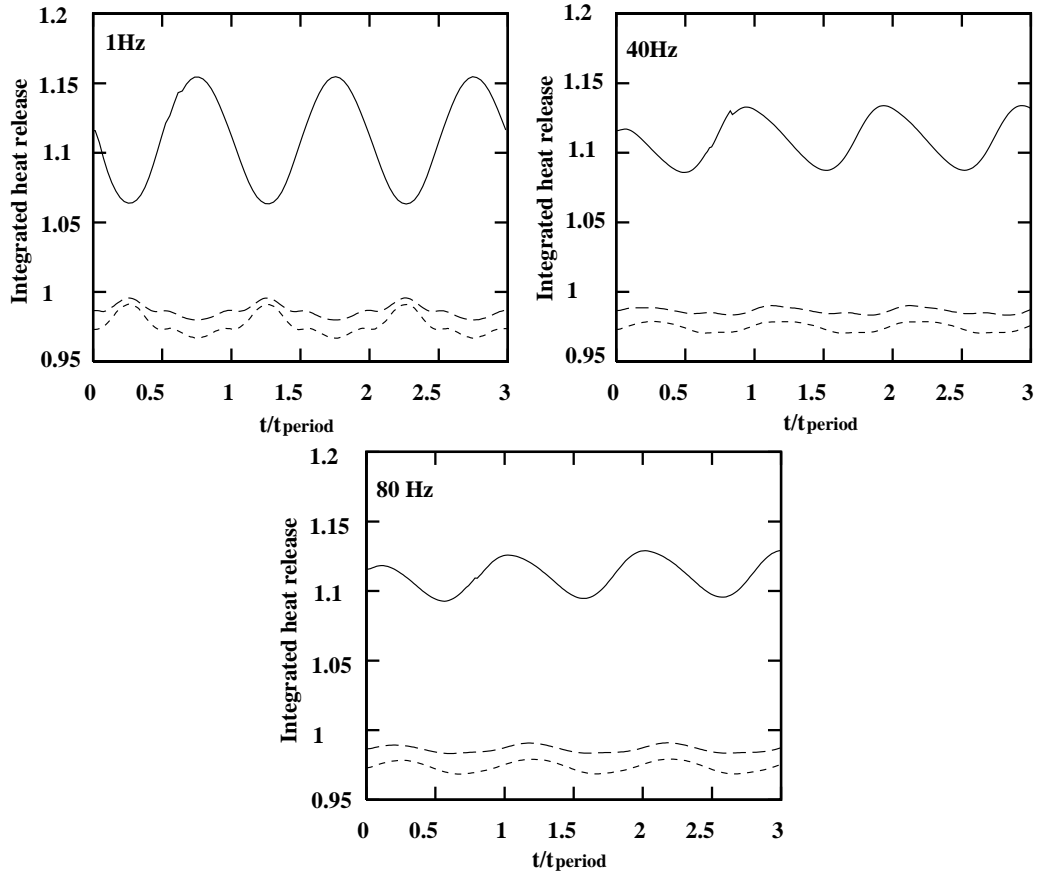


FIGURE 10. Evolution of the heat release integrated across the flame front (reduced by the unstrained value) in function of time ( $Le_A = 1.0$ ). — : GRI-mech; ---- : one-step mechanism; ..... : two-step mechanism.

This behavior is well summarized on Fig. 11, in which the scatter plot of the heat release rate versus the strain rate is represented for all the frequencies (1, 40, and 80 Hz). Very clear correlations are observed, and different signs for the slopes are found between the cases  $Le_A = 0.95$  and  $Le_A = 1.0$ .

This seems to indicate that the thermo-diffusive properties of the mixture is a first order parameter in the behavior of strained laminar flames.

#### 4. Vortex-premixed laminar flame interaction

The configuration investigated here concerns the interaction between a two-dimensional vortex pair generated by acoustic excitation and a V-shaped air-methane premixed laminar flame stabilized on a heated wire. A counter-rotating vortex pair propagating itself by mutual induction interacts with an initially planar premixed flame. Figure 12 shows the vorticity and heat release fields during the interaction ( $t = 5\text{ms}$ ). Here, the Lewis number based on the reactants is taken equal to unity. This problem has been extensively studied both experimentally (Samaniego *et al.* 1996) and numerically (Mantel 1994). Here, a lean methane-air flame is investigated (equivalence ratio = 0.55). The initial conditions for the simulations are obtained from the

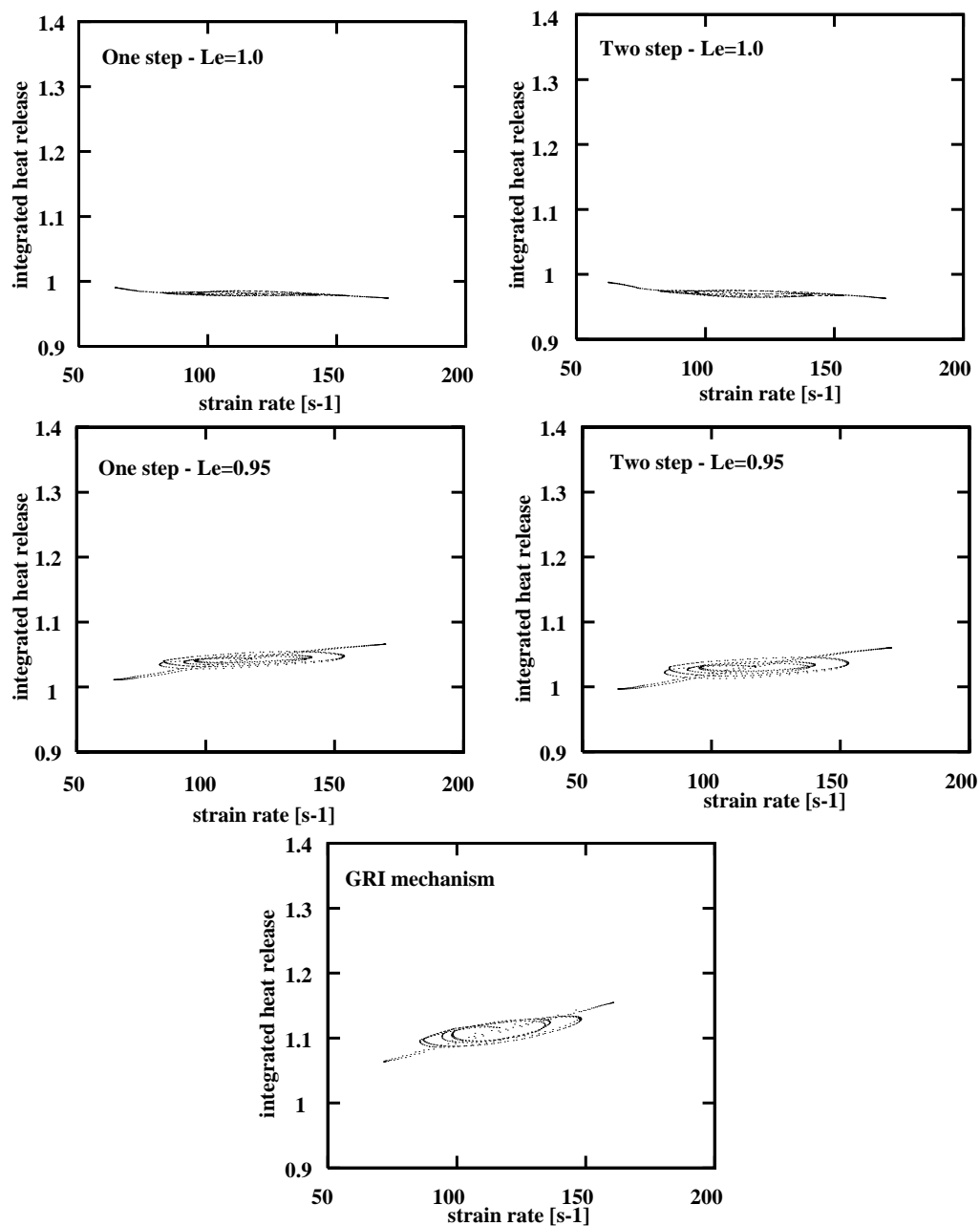


FIGURE 11. Scatter plot of the integrated heat release across the flame front (reduced by the unstrained value) vs strain rate.

experiment. The characteristics of the interaction are  $V_D/S_L = 66.8$ ,  $s/\delta_f = 25.7$ , and  $D/\delta_f = 104.8$ , where  $V_D$ ,  $S_L$  represent respectively the displacement velocity of the vortex pair and the laminar burning velocity; and  $s$ ,  $\delta_f$ , and  $D$  are the distance between the center of the vortices, the laminar flame thickness, and the distance separating the vortex pair from the laminar flame.

Details concerning the geometry and diagnostic techniques can be found in Samaniego *et al.* (1996). Information concerning the equations solved in the DNS code and

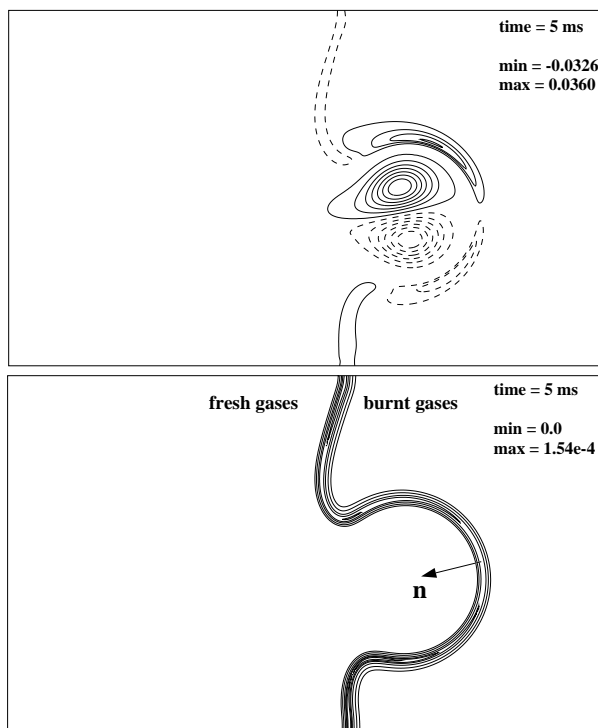


FIGURE 12. Vorticity (top) and heat release rate (bottom) fields at  $t = 5$ ms of the interaction (from Mantel *et al.* 1996).

the computational configuration are presented in Mantel (1994).

Since radiative heat losses effects have been found negligible during this interaction (Samaniego 1996, Mantel 1994), adiabatic conditions for the flame are taken for the simulations. Figure 13 shows the time evolution of the flame length (non-dimensionalized by its initial length). Comparison with the experimental results of Samaniego (1996) points out that the dynamic of the interaction is well reproduced by the simulations. The time evolution of the minimum heat release rate integrated along a normal to the flame and encountered along the flame is also shown Fig. 13. As long as the interaction goes on, the vortex pair increases the flame length and leads to a decrease of the heat release rate at a location in front of the vortex pair. This is qualitatively well described both by one- and two-step mechanism. In this configuration, the two-step model allows a significant improvement in the description of the decrease of the heat release rate.

## 5. Conclusions

This paper presents a new methodology to determine kinetic parameters of one- and two-step chemical models classically used in DNS of premixed combustion. By using a one-dimensional code in which simple chemical models and simple transport properties are implemented, the kinetic parameters are determined in order to verify (1) the laminar burning velocity, (2) the temperature and concentration profiles, and (3) the extinction strain rate of a laminar flame in the opposed jet configuration (counterflow flames). To do so, the results issued from these simple models are

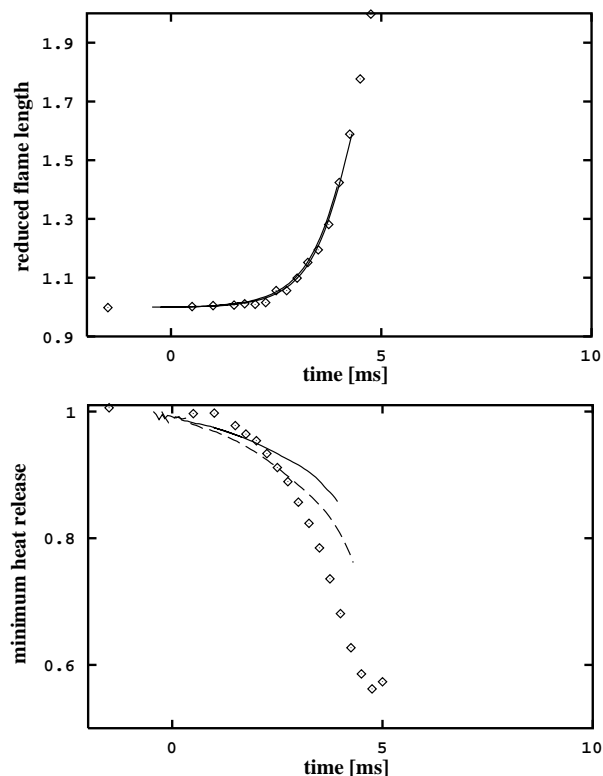


FIGURE 13. Time evolution of the flame length (top) and minimum heat release rate integrated across the flame. — : one-step mechanism; ---- : two-step mechanism.

compared in detail with results obtained from the GRI-mech 2.1 mechanism and multi-component transport properties.

Applications of these simple mechanisms and transport models on two unsteady configurations show good behavior of these models. In the case of a flame submitted to an unsteady strain, both one- and two-step models describe qualitatively well the dynamic of the flame and the heat release amplitude for different frequencies. In this configuration, no obvious improvement is obtained with the two-step model. However, the Lewis number based on the reactant seems to be a determining parameter for laminar strained flames. A slight variation of the Lewis number from 0.95 to 1.0 leads to a completely different behavior of the flame.

The interaction between a two-dimensional vortex pair with an initially planar premixed flame is also analyzed by DNS using the one- and two-step chemical models. In this case, comparisons with the experimental results of Samaniego *et al.* (1996) shows that the two-step chemical model allows a better description of the interaction. However, further work is needed to investigate the effects of a slight variation of the Lewis number on the behavior of the flame during the vortex-flame interaction.

This methodology can be improved by studying a configuration of laminar strained

flame more representative of turbulent premixed flames. This concerns the counterflow flame configuration, but with hot products on one side and reactants on the other side. Further work is in progress to examine the behavior of simple and transport models.

### Acknowledgments

The authors wish to thank Dr. Jean-Michel Samaniego for his encouraging and fruitful support.

### REFERENCES

- CHEN, J. H., MAHALINGAM, S., PURI, I. K., & VERVISCH, L. 1992 Structure of turbulent non-premixed flames modeled with two-step chemistry. In *Proc. 1992 Summer Program*, Center for Turbulence Research, NASA Ames/Stanford Univ. 389-402.
- CHUNG, S. H., KIM, J. S. & LAW, C. K. 1986 Extinction of interacting premixed flames: Theory and experimental comparisons. *21st Symp. (Int'l.) on Combust.* The Combustion Institute. 1845-1851.
- CLAVIN, P. 1985 Dynamic behavior of premixed flame fronts in laminar and turbulent flows. *Progress in Energy and Combustion Science.* **11**, 1-59.
- EGOLFOPOULOS, F. N. 1994a Dynamics and structure of unsteady, strained, laminar premixed flames. *25th Symp. (Int'l.) on Combust.* The Combustion Institute. 1365-1373.
- EGOLFOPOULOS, F. N. 1994b Geometric and radiation effects on steady and unsteady strained laminar flames. *25th Symp. (Int'l.) on Combust.* The Combustion Institute. 1375-1381.
- FRENKLACH, M., WANG, H., GOLDENBERG, M., SMITH, G. P., GOLDEN, D. M., BOWMAN, C. T., HANSON, R. K., GARDINER, W. C. & LISSIANSKI, V. 1995 GRI-Mech - An optimized detailed chemical reaction mechanism for methane combustion. *Gas Research Institute report GRI-95/0058.*
- GLASSMAN, I. 1987 *Combustion.* Academic Press 2nd Ed.
- HILKA, M., VEYNANTE, D., BAUM, M. & POINSOT, T. 1995 Simulation of flame-vortex interactions using detailed and reduced chemistry. *10th Symposium on Turbulent Shear Flows.*
- KEE, R. J., GRGAR, J. F., SMOOKE, M.D. & MILLER, J. A. 1994 A fortran program for modeling steady laminar one-dimensional premixed flames. *Sandia National Laboratories - SAND85-8240.*
- KEE, R. J., RUPLEY, F. M. & MILLER, J. A. 1989 Chemkin-II: A fortran chemical kinetics package for the analysis of gas phase chemical kinetics. *Sandia National Laboratories - SAND89-8009B.*
- LAW, C. K. 1988 Dynamics of Stretched Flames. *22nd Symp. (Int'l.) on Combust.* The Combustion Institute. 1381-1402.

- LAW, C. K., ZHU, D. L. & YU, G. 1986 Propagation and extinction of stretched premixed flames. *21st Symp. (Int'l.) on Combust.* The Combustion Institute. 1419-1426.
- LIÑÁN, A. 1974 A Theoretical analysis of premixed flame propagation with an isothermal chain reaction. Instituto Nacional De Tecnica Aeroespacial, Esteban Terradas, Madrid, Spain.
- MANTEL, T. 1994 Fundamental Mechanisms in Premixed Flame Propagation Via Vortex Flame Interactions-Numerical Simulations. *Annual Research Briefs*. Center for Turbulence Research, NASA Ames/Stanford Univ. 45-75.
- MANTEL, T., SAMANIEGO, J.-M., & BOWMAN, C. T. 1996 Fundamental mechanisms in premixed flame propagation via vortex flame interactions-Part II: Numerical Simulations. *In preparation*.
- POINSOT, T. 1996 Using direct numerical simulations to understand premixed turbulent combustion. *26th Symp. (Int'l.) on Combust.* The Combustion Institute.
- POINSOT, T., CANDEL, S., & TROUVÉ, A. 1996 Applications of direct numerical simulation to premixed turbulent combustion. *Progress in Energy and Combustion Science*. **21**, 531-576.
- POINSOT, T., VEYNANTE, D. & CANDEL, S. M. 1991 Quenching processes and premixed turbulent combustion diagrams. *J. Fluid Mech.* **228**, 561-605.
- RUTLAND, C. J., 1989 Effects of strain, vorticity and turbulence on premixed flames. *Ph-D Thesis*, Stanford University.
- RUTLAND, C. J. & TROUVÉ, A. 1993 Direct simulations of premixed turbulent flames with non-unity Lewis numbers. *Combust. Flame*. **94**, 41-57.
- SAMANIEGO, J.-M., MANTEL, T. & BOWMAN, C. T. 1996 Fundamental mechanisms in premixed flame propagation via vortex flame interactions-Part I: Experiment. Submitted to *J. Fluid Mech.*
- SESHADRI, K. & PETERS, N. 1983 The influence of stretch on a premixed flame with two-step kinetics. *Combust. Sci. Tech.* **22**, 119-129.
- TROUVÉ, A. & POINSOT, T. 1994 The evolution equation for the flame surface density in turbulent premixed combustion. *J. Fluid Mech.* **278**, 1-31.
- VERVISCH, L. 1992 Study and Modeling of finite rate chemistry effects in turbulent non-premixed flames. *In Annual Research Briefs* Center for Turbulence Research, NASA Ames/Stanford Univ. 411-429.
- WILLIAMS, F. A. 1985 *Combustion theory*. 2nd ed., Benjamin Cummings.
- ZEL'DOVICH, Y. B. 1948 Theory of flame propagation. *Zhur. Fizi. Khi. (USSR)*. **22**, 27-49.